Contribution from the Departments of Chemistry, Calfornia State University—Sacramento, Sacramento, California 95819, Wayne State University, Detroit, Michigan 48202, and Northeastern University, Boston, Massachusetts 02115

Synthesis and Characterization of a Hydroxyl-Bridged Iron(III) Dimer of *N,N'*-Ethylenebis(salicylamine)

LONDA BORER,* LINDA THALKEN, CHRISTOPHER CECCARELLI, MILTON GLICK, JIAN HUA ZHANG, and WILLIAM MICHAEL REIFF

Received April 5, 1982

A number of investigations have implicated a binuclear complex, $[FeOH]_2^{4+}$, as the predominant hydrolysis species in solutions of iron(III). We have prepared a complex of formula $[FeLOH]_2 \cdot 2H_2O \cdot 2py$, where L = *N,N'*-ethylenebis(salicylamine). The red crystal was determined to have a monoclinic unit cell of space group $P2_1/c$ and $a = 7.073$ (3) Å, $b = 19.421$ (7) Å, $c = 15.564$ (9) Å, $\beta = 9.48$ (5)°, and $d_{obsd} = 1.39$ g/cm³. Least-squares refinement of 1423 reflections gave an *R* factor of 0.065. The structure consists of centrosymmetric dimer units in which crystallographically equivalent iron(III) ions are bridged by hydroxyl groups. The planar $[FeOH]_2^{4+}$ unit has an Fe–OH–Fe bridging angle of 102.8 (3)°. The nonequivalent Fe–OH distances of 2.055 (6) and 1.986 (6) Å reflect the influence of the two nitrogen atoms of the tetradentate ligand. Water and pyridines of crystallization are hydrogen bonded to the bridging hydroxyl ions. The EPR powder spectrum at 298 K reveals a broad signal centered at $g = 2.02$. The magnetic susceptibility was measured over the 80–373 K range. With use of the spin–spin coupling model for an $S_1 = S_2 = {}^5/_2$ system and $g = 2.02$, $\Theta = 0$ K, and $N\alpha = 0$, the exchange integral, *J*, was determined to be -10.4 cm^{-1} for the crystal, which is indicative of antiferromagnetism.

Introduction

Many of the functions of iron in biological systems depend upon the aqueous chemistry of iron(III) and are apparently dominated by hydrolysis and polymerization. The dihydroxy-bridged iron(III) dimer

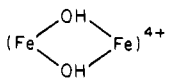

has been implicated as being the major hydrolytic species of iron in solution.[1] We report here the preparation and characterization of a dihydroxy-bridged iron(III) complex of formula $[FeLOH]_2$ and the crystalline structure of $[FeLOH]_2 \cdot 2H_2O \cdot 2py$, where L = *N,N'*-ethylenebis(salicylamine). The ligand has the structure given in Figure 1. This ligand is similar to the Schiff base *N,N'*-ethylenebis(salicylideneamine) referred to in the literature as salen, in that it is tetradentate and contains the same donating atoms, N_2O_2; however, the ligand used here contains saturated nitrogen atoms and greater flexibility in the ligand would be expected. A variety of bridged iron(III) complexes of the Schiff base have been characterized,[2-5] but to our knowledge no iron(III) complexes have been reported of the ligand used in this study.

Experimental Section

(1) Preparation of the Ligand and Complexes. The ligand was prepared by the condensation of salicylaldehyde and ethylenediamine, and the hydrogenation was carried out as described by Freedman.[6] The procedures used for the preparation of the title compound are those of Niswander and Martell.[7] The ligand (1.4 g, 5 mmol) was dissolved in a solution of 15 mL of *n*-propyl alcohol and 25 mL of pyridine and heated in a 250-mL round-bottom flask. $FeSO_4 \cdot 7H_2O$ (1.4 g, 5 mmol) was dissolved in 15 mL of water and slowly added to the hot ligand solution. The resulting dark brown solution was stirred and allowed to reflux for 30 min. After the solution was cooled, an orange powdery solid was collected and washed with a 50/50 solution of *n*-propyl alcohol and water. The product yield was increased substantially, however, if additional water was added to the solution before collecting the precipitate. Anal. Calcd for $[Fe(C_{16}H_{18}N_2O_2)OH]_2$: C, 55.99; H, 5.58; N, 8.16; Fe, 16.27. Found: C, 55.33; H, 5.69; N, 8.13; Fe, 15.91. The molecular weight was calculated as 686.88 and was found to be 692 in DMF by vapor pressure osometry. The orange solid was recrystallized by dissolving it in a minimum amount of pyridine and allowing this solution to stand under an atmosphere of acetone vapors undisturbed for 2–3 weeks. The orange needles were collected and dried in a vacuum; mp 275 °C dec. Anal. Calcd for $[Fe(C_{16}H_{18}N_2O_2)OH]_2 \cdot 2H_2O \cdot 2py$: C, 57.3; H, 5.95; N, 9.55; Fe, 12.69. Found: C, 57.5; H, 6.16; N, 8.93; Fe, 12.82. If this preparation was carried out with an anhydrous salt of iron(III), a purple complex was formed with a formula of FeLX(py), where L is the ligand and X is the anion of the iron(III) salt used. Since no water was present in the reaction, a hydroxy dimer was unable to form. The various purple complexes are presumed to be monomeric; however, none were obtained in a pure state, and therefore, no further characterization was done.

(2) Crystal Structure Determination. A crystal of dimensions 0.21 × 0.11 × 0.11 mm of the iron dimer was mounted on a Syntex $P2_1$ diffractometer. Axial photographs showed the diffraction symmetry to be $2/m$. The unit cell dimensions and their standard deviations were obtained by least-squares refinement based upon the 2θ values of reflections. They are as follows ($\lambda = 0.71069$ Å): $a = 7.073$ (3) Å, $b = 19.421$ (9) Å, $c = 15.564$ (9) Å, $\beta = 99.45$ (5)°. Reflection intensities were measured in one quadrant of reciprocal space for $2\theta \leq 45°$ with use of the $\theta/2\theta$ step scan technique. Lorentz–polarization corrections were made in the usual way; no absorption corrections ($\mu_{Mo K\alpha} = 7.43$ cm^{-1}) were applied to the data. A total of 2790 independent data was processed, of which 1423 had $I \geq 2.56(I)$.

An examination of the data revealed systematic absences consistent with space group $P2_1/c$. An F^2 Patterson synthesis revealed the position of the iron atom. An iron-phased F_o synthesis brought out the rest of the structure, excepting the oxygen of the water of crystallization. The oxygen appeared in a subsequent $F_o - F_c$ synthesis. Hydrogen positions were calculated by assuming C–H bond distances of 1.09 Å and included in the structural mode. The hydroxyl hydrogen and the hydrogens of the water of crystallization were not included. Anisotropic full-matrix least-squares refinement of this model resulted in $R(F) = 0.061$, $R_w(F^2) = 0.065$, and $S = 1.44$.

Tables of hydrogen positions, thermal parameters, and structure factors have been deposited as supplementary material.

(3) Instrumentation. All infrared spectra were measured on a Perkin-Elmer 598 IR spectrophotometer as KBr pellets. A reaction using D_2O instead of H_2O as the precipitating agent gave us the deuterated complex. The EPR spectrum was obtained on a Varian E-4 instrument using DPPH as the standard.

Variable-temperature magnetic susceptibility data were obtained with use of samples approximately 10 mg in size by the Faraday method. Liquid nitrogen was used as the cryogenic material to obtain the low-temperature readings to ~80 K. Details of the Mössbauer

*To whom correspondence should be addressed at California State University—Sacramento.

(1) Webb, J. "Techniques and Topics in Bioinorganic Chemistry"; McAuliffe, C. A., Ed.; Wiley: New York, 1975; pp 270–304.
(2) Holm, R. H.; Everett, G. W.; Chakravorty, A. *Prog. Inorg. Chem.* **1966**, *7*, 83–214.
(3) Gerloch, M.; McKenzie, E. P.; Towl, A. D. C. *J. Chem. Soc. A* **1969**, 2850.
(4) Lewis, J.; Mabbs, F. E.; Richards, A. *J. Chem. Soc. A* **1967**, 1014.
(5) Gerloch, M.; Lewis, J.; Mabbs, F. E.; Richards, A. *J. Chem. Soc. A* **1968**, 112.
(6) Freedman, H. H. *J. Am. Chem. Soc.* **1961**, *83*, 2900.
(7) Niswander, R. H.; Martell, A. E. *Inorg. Chem.* **1978**, *17*, 2341.

0020-1669/83/1322-1719$01.50/0

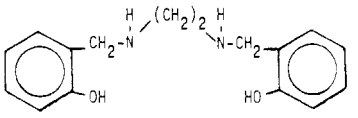

Figure 1. Structure of *N,N'*-ethylenebis(salicylamine).

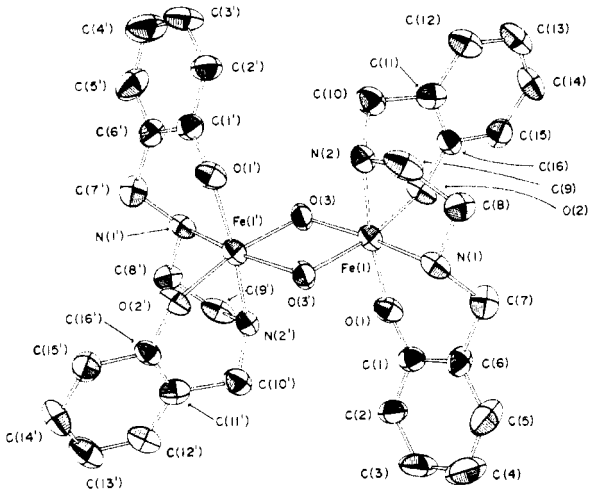

Figure 2. Fe dimer at 298 K. The thermal ellipsoids are at 50% probability. The primed and unprimed atoms are related by a center of symmetry.

Table I. Atomic Coordinates for the Iron Dimer[a]

	x	*y*	*z*
Fe(1)	0.04680 (19)	−0.04998 (8)	0.08058 (9)
O(1)	0.1568 (9)	−0.1269 (4)	0.0235 (4)
O(2)	0.2324 (8)	−0.0526 (4)	0.1850 (4)
O(3)	0.1605 (9)	0.0278 (3)	0.0245 (4)
N(1)	−0.1540 (10)	−0.1238 (4)	0.1219 (5)
N(2)	−0.1273 (11)	0.0176 (4)	0.1512 (5)
C(1)	0.0762 (13)	−0.1871 (5)	−0.0012 (6)
C(2)	0.1068 (15)	−0.2180 (5)	−0.0786 (7)
C(3)	0.0345 (18)	−0.2816 (6)	−0.1037 (7)
C(4)	−0.0779 (19)	−0.3171 (6)	−0.0524 (9)
C(5)	−0.1108 (17)	−0.2869 (6)	0.0241 (8)
C(6)	−0.0379 (14)	−0.2235 (5)	0.0509 (6)
C(7)	−0.0675 (14)	−0.1933 (5)	0.1361 (6)
C(8)	−0.2202 (13)	−0.0956 (5)	0.2004 (6)
C(9)	−0.2846 (14)	−0.0219 (6)	0.1828 (6)
C(10)	−0.0115 (13)	0.0606 (6)	0.2180 (6)
C(11)	0.1030 (14)	0.0178 (5)	0.2902 (7)
C(12)	0.1010 (15)	0.0322 (6)	0.3769 (7)
C(13)	0.2174 (18)	−0.0034 (7)	0.4421 (7)
C(14)	0.3398 (16)	−0.0525 (7)	0.4215 (6)
C(15)	0.3467 (14)	−0.0685 (5)	0.3357 (7)
C(16)	0.2267 (13)	−0.0340 (5)	0.2674 (6)
N(P1)	0.4814 (12)	0.1776 (5)	0.1918 (6)
C(P1)	0.4731 (15)	0.1257 (6)	0.2468 (7)
C(P2)	0.5379 (16)	0.2416 (7)	0.2255 (7)
C(P3)	0.5175 (18)	0.1334 (7)	0.3378 (8)
C(P4)	0.5815 (16)	0.2543 (6)	0.3151 (7)
C(P5)	0.5743 (18)	0.1986 (7)	0.3708 (8)
O(WC)	0.4861 (10)	0.1143 (3)	0.0259 (4)

[a] Estimated standard deviations given in parentheses refer to the least significant digits.

spectrometer have been reported previously.[8]

Results

(1) Description of the Crystal Structure. The orange-red crystal of formula $[FeLOH]_2 \cdot 2H_2O \cdot 2py$ was determined to have a monoclinic unit cell of space group $P2_1/c$ and d_{obsd} = 1.39 g/cm^3. The atomic coordinates for the dimer are given in Table I. The structure consists of centrosymmetric dimer units in which crystallographically equivalent iron(III) ions are bridged by hydroxyl groups. The structure is shown in Figure 2. The ligand with N_2O_2 donating atoms occupies four coordination sites of the iron(III) while the two remaining sites are filled by the bridging hydroxyl groups. The iron(III) ions have distorted-octahedral coordination geometry as evidenced particularly by the angle O(1)–Fe(1)–N(2) of 166.1°. (Refer to Table II for the bond angles). The distortion is further demonstrated by deviations from the least-squares planes as shown by the torsion angles given in Table III. The $[FeOH]_2^{4+}$ unit lies on a plane. The two benzene rings of the

(8) Wong, H.; Chang, C.; Reiff, W. M. *Inorg. Chem.* **1977**, *16*, 819.

Table II. Bond Angles for the Fe Dimer[a]

atom 1	atom 2	atom 3	angle, deg
	Bridging		
Fe(1)	O(3)	Fe(1′)	102.8 (3)
O(3)	Fe(1)	O(3′)	77.2 (3)
	Coordination around the Iron Atom		
O(2)	Fe(1)	O(1)	95.5 (3)
O(2)	Fe(1)	O(3)	97.1 (3)
O(2)	Fe(1)	O(3′)	168.9 (3)
O(2)	Fe(1)	N(1)	96.9 (3)
O(2)	Fe(1)	N(2)	87.3 (3)
O(1)	Fe(1)	O(3)	99.3 (2)
O(1)	Fe(1)	N(1)	87.6 (3)
O(1)	Fe(1)	N(2)	166.1 (3)
O(3)	Fe(1)	N(1)	163.7 (3)
O(3)	Fe(1)	N(2)	93.8 (3)
	Water and Pyridine of Crystallization		
O(1*)	OW(1)	O(3)	145.5 (3)
O(1*)	OW(1)	NP(1)	111.0 (3)
O(3)	OW(1)	NP(1)	97.5 (3)

[a] Coordinates marked with a prime are at $-x, -y, -z$; those marked with an asterisk are at $1-x, -y, -z$.

Table III. Characteristics of Rings in the Structure

atom 1	atom 2	atom 3	atom 4	torsion angle, deg
(1) Plane Defined by Fe(1)–O(1)–C(1)–C(6)–C(7)–N(1)				
N(1)	Fe(1)	O(1)	C(1)	−21.0 (7)
O(1)	Fe(1)	N(1)	C(7)	−31.2 (6)
Fe(1)	N(1)	C(7)	C(6)	+68.5 (9)
Fe(1)	O(1)	C(1)	C(6)	+40.2 (12)
O(1)	C(1)	C(6)	C(7)	+0.2 (14)
C(1)	C(6)	C(7)	N(1)	−57.4 (11)
(2) Plane Defined by Fe(1)–N(1)–C(8)–C(9)–N(2)				
N(2)	Fe(1)	N(1)	C(8)	+24.1 (6)
N(1)	Fe(1)	N(2)	C(9)	+2.7 (6)
Fe(1)	N(1)	C(8)	C(9)	−49.6 (8)
Fe(1)	N(2)	C(9)	C(8)	−29.8 (9)
N(1)	C(8)	C(9)	N(2)	+52.9 (9)
(3) Plane Defined by Fe(1)–N(2)–C(10)–C(11)–C(16)–O(2)				
N(2)	Fe(1)	O(2)	C(16)	−13.4 (8)
O(2)	Fe(1)	N(2)	C(10)	−30.5 (6)
Fe(1)	O(2)	C(16)	C(11)	+26.9 (13)
Fe(1)	N(2)	C(10)	C(11)	+63.4 (8)
N(2)	C(10)	C(11)	C(16)	−54.9 (11)
C(10)	C(11)	C(16)	O(2)	+7.8 (13)
(4) Plane Defined by C(1)–C(2)–C(3)–C(4)–C(5)–C(6)				
C(6)	C(1)	C(2)	C(3)	+1.4 (16)
C(2)	C(1)	C(6)	C(5)	−0.6 (15)
C(1)	C(2)	C(3)	C(4)	−1.7 (19)
C(2)	C(3)	C(4)	C(5)	+1.1 (20)
C(3)	C(4)	C(5)	C(6)	−0.3 (20)
C(4)	C(5)	C(6)	C(1)	+0.1 (18)
(5) Plane Defined by C(11)–C(12)–C(13)–C(14)–C(15)–C(16)				
C(16)	C(11)	C(12)	C(13)	+0.3 (16)
C(12)	C(11)	C(16)	C(15)	+0.9 (13)
C(11)	C(12)	C(13)	C(14)	−1.4 (18)
C(12)	C(13)	C(14)	C(15)	+1.3 (18)
C(13)	C(14)	C(15)	C(16)	−0.1 (17)
C(14)	C(15)	C(16)	C(11)	−1.0 (14)

Table IV. Bond Lengths for $[FeLOH]_2 \cdot 2H_2O \cdot 2py$

atom 1	atom 2	bond length, Å	atom 1	atom 2	bond length, Å
Fe(1)	Fe(1′)	3.155 (3)	Fe(1)	N(1)	2.188 (8)
Fe(1)	O(2)	1.915 (6)	Fe(1)	N(2)	2.212 (8)
Fe(1)	O(1)	1.964 (7)	OW(1)	O(3)	2.847 (9)
Fe(1)	O(3)	1.986 (6)	OW(1)	NP(1)	2.865 (11)
Fe(1)	O(3′)	2.055 (6)			

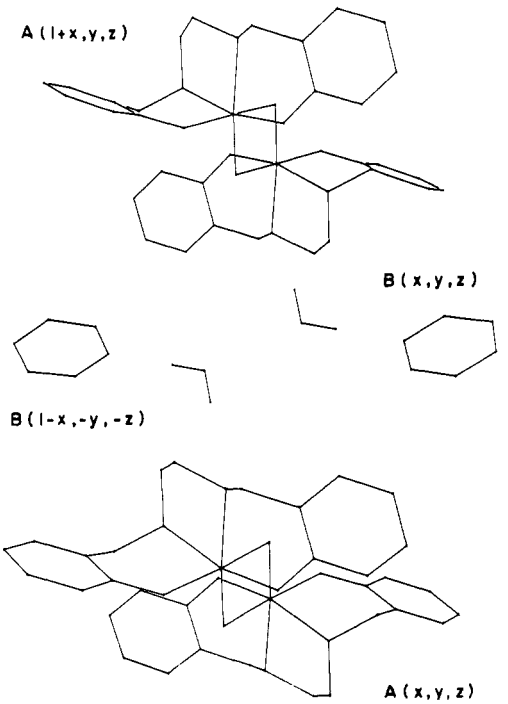

Figure 3. Crystal packing structure of the Fe dimer at 298 K. Molecules A are the Fe dimer; molecules B are the pyridine and water of crystallization. The scale along *a* has been expanded for clarity.

ligand also lie in a plane but in a different one from the iron bridging unit. The Fe–OH–Fe bridging angle in the planar unit is 102.8 (3)°.

Bond distances are given in Table IV. The Fe···Fe separation of 3.155 (3) Å is large enough so that significant direct overlap of metal ion orbitals based on the ionic radius (0.65–0.79 Å) of high-spin six-coordinate Fe(III) is not expected.[9] This distance is slightly larger than the values reported by Schugar for two dihydroxyl iron(III) complexes: $[Chel(H_2O)FeOH]_2 \cdot 4H_2O$ (3.078 Å) and $[Dipic(H_2O)FeOH]_2$ (3.089 Å).[10]

Individual dimeric units are separated from each other by a water and a pyridine of crystallization as shown in the packing diagram in Figure 3. The individual dimers can therefore be considered virtually magnetically dilute. The O–H···O distance of 2.847 (9) Å observed between the hydroxyl bridge and the water of crystallization is well within the range of possible hydrogen bonding.[11]

(2) Infrared Spectra. In the ligand the phenolic hydroxyl group is intramolecularly bonded to a nitrogen.[6] The OH stretching frequency for this group is in the 3200–2500-cm^{-1} region of the spectrum and disappears upon chelation. A peak observed in the spectrum of the iron complex at ~3600 cm^{-1} is assigned to the bridging OH stretch and the strong band from 3500 to 3000 cm^{-1} (centered at ~3420 cm^{-1}) is assigned to the OH stretching modes of the water of crystallization, or lattice water, hydrogen bonded to the bridging OH group. The NH stretching mode is observed at ~3300 cm^{-1} in the ligand. Two different types of nitrogen atoms are observed in the crystalline complex; consequently the peaks at 3280 and 3270 cm^{-1} are assigned to the free NH and the hydrogen-bonded NH, respectively. Upon deuteration of the iron complex, three broad peaks are observed in the 2300–2600-cm^{-1} region: one centered at ~2380 cm^{-1}, another at ~2400 cm^{-1}, and a third at ~2550 cm^{-1}. Since the hydrogen on the ligand nitrogen would be expected to exchange in the presence of D_2O, one of these bands will be assigned to the N–D stretch. With use of the fact that deuteration results in an isotopic red shift of $\sim 2^{1/2}$, these peaks are assigned to N–D and O–D of the lattice water and O–D of the bridging group, respectively.

The region of the infrared spectra from 1000 to 300 cm^{-1} for crystalline $[FeLOH]_2$ and the deuterated complex are shown in Figure 4. Of particular significance in this region is the peak at 880 cm^{-1} in the complex, which disappears upon deuteration, and a new peak at 621 cm^{-1}, which is observed in the spectrum of the deuterated complex. Therefore, we have assigned the 880-cm^{-1} peak to the OH bridging deformation and the peak at 621 cm^{-1} in the deuterated spectrum to the O–D bridging deformation. Other new peaks that arise in this region of the spectrum can be attributed to the deuteration of the N–H bond in the ligand.

Table V. Magnetic Susceptibility Data for $[FeLOH]_2$ and $[FeLOH]_2 \cdot 2H_2O \cdot 2py$[a]

	$[FeLOH]_2$		$[FeLOH]_2 \cdot 2H_2O \cdot 2py$	
T, K	$10^{-2}\chi_{cor}$	μ_{eff}, μ_B	$10^{-2}\chi_{cor}$	μ_{eff}, μ_B
80	3.270	4.59	1.653	3.41
128	2.191	4.76	1.633	4.11
153	2.061	5.04	1.538	4.36
198	1.721	5.24	1.272	4.51
233	1.470	5.26	1.250	4.85
273	1.347	5.45	1.201	5.14
296	1.285	5.54	1.106	5.17
323	1.140	5.45		
343	1.045	5.38		
373	0.960	5.37		

[a] $\chi_d = -96.62 \times 10^{-6}$ cgsu/Fe(III) for $[FeLOH]_2$ based on Pascal's constants. $\chi_d = -109.04 \times 10^{-6}$ cgsu/Fe(III) for $[FeLOH]_2 \cdot 2H_2O \cdot 2py$. μ_{eff} was calculated by using $\mu_{eff} = 2.84 (\chi_{cor}T)^{1/2}$.

Table VI. Mössbauer Spectroscopy Parameters[a] for $[FeLOH]_2 \cdot 2H_2O \cdot 2py$

T, K	δ	ΔE	Γ_1	Γ_2	Γ_1/Γ_2	A_1/A_2
300	0.387	0.539	0.553	0.667	0.829	1.20
100	0.430	0.563	0.506	0.621	0.815	1.11
4.3	0.494	0.561	0.344	0.341	1.01	1.02
1.9	0.495	0.560	0.381	0.375	1.02	1.02

[a] In mm/s relative to 6.4 μm thick natural iron foil.

(3) Magnetic Data. The EPR spectrum of the powder sample at 25 °C reveals a broad signal at $g = 2.02$. This broadening of the signal is expected because of the closeness of the magnetic ions. The magnetic susceptibility data for the two samples, $[FeLOH]_2$ and $[FeLOH]_2 \cdot 2H_2O \cdot 2py$, in the range of 80–373 K corrected for diamagnetism, χ_d, are presented per Fe(III) in Table V. With use of the spin–spin coupling model for an $S_1 = S_2 = {}^5/_2$ system and $g = 2.02$, $\theta = 0$ K, and $N\alpha = 0$, the following relationship was used to calculate J, the exchange integral:

$$\chi_m = [g^2\beta^2 N \exp(2x) + 5\exp(6x) + 14\exp(12x) + 30\exp(20x) + 55\exp(30x)]/[(k(T-\theta))[1 + 3\exp(2x) + 5\exp(6x) + 7\exp(12x) + 9\exp(20x) + 11\exp(30x)]] + N\alpha$$

(9) Shannon, R. D.; Prewitt, C. T. *Acta Crystallogr., Sect. B* **1969**, *B25*, 925.
(10) Thich, J. A.; Ou, C. C.; Powers, D.; Vasiliou, B.; Mastropaolo, D.; Potenza, J. A.; Schugar, H. J. *J. Am. Chem. Soc.* **1976**, *98*, 1425.
(11) Stout, G.; Jensen, L. "X-Ray Structure Determination", Macmillan: Toronto, 1968; p 303.

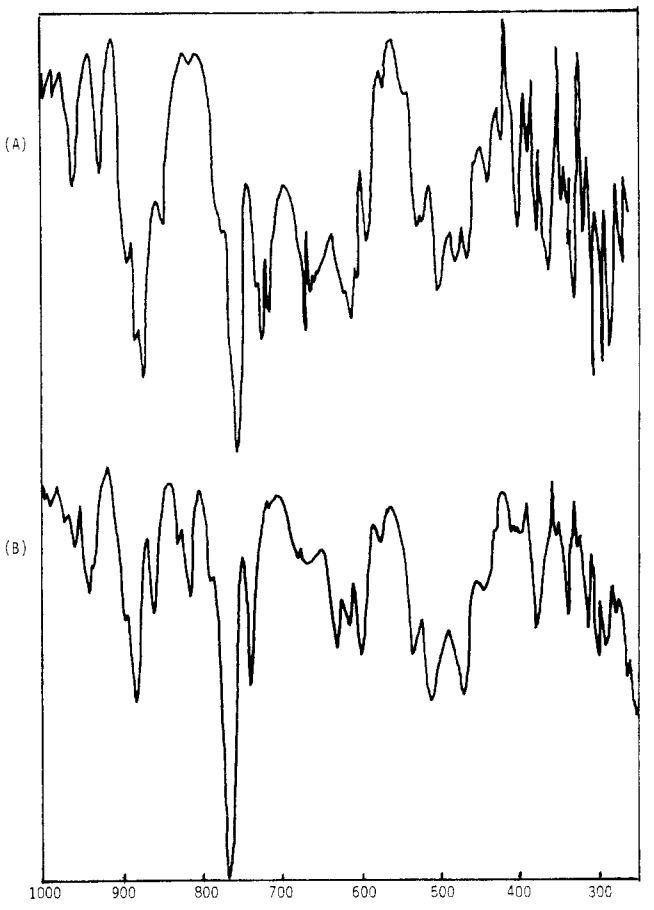

Figure 4. IR spectra for (A) the Fe(III) hydroxyl-bridged dimer and (B) the deuterated complex from 1000 to 300 cm^{-1}.

where $x = -J/kt$ and Θ = Weiss constant.

The average J values calculated were -6.9 cm^{-1} for $[FeLOH]_2$ and -10.4 cm^{-1} for the crystalline complex.

(4) Mössbauer Spectra. The temperature dependence of the Mössbauer spectra of $[FeLOH]_2 \cdot 2H_2O \cdot 2py$ is shown in Figure 5, and pertinent parameters are given in Table VI. The isomer shift is characteristic of spin-sextet ferric ions and reasonable for a pseudooctahedral FeN_2O_4 chromophore. The spectra at all temperatures can be fit to a single quadrupole doublet, indicating electronically equivalent metal ions consistent with the X-ray results. The magnitude of the quadrupole splitting is *small* and more like that typical of *monomeric* high-spin iron(III).[12] The observed value is to be compared to the substantially larger splittings found[13] for the related dimers $[Fe(salen)]_2O$ (0.78 mm/s at 77 K) and $[Fe(salen)Cl]_2$ (1.40 mm/s at 77 K). The larger electric field gradients[14] in these systems arise from the strong (partial double) Fe–O bonds (1.77–1.81 Å) in the former[15] and axial chlorine atoms in the latter. The electric field gradient arising from the "normal" Fe^{III}–Cl bonds (2.294 Å) is apparently not balanced out by that arising from the weak Fe–O bonds (2.178 Å)[16] that hold the $[Fe(salen)Cl]_2$ "dimers" together.

The temperature dependence of the spectrum clearly confirms the antiferromagnetic coupling and total spin (S_T) = 0 ground state for the system. In view of $J = -10.8$ cm^{-1} from the fit to χ'_M vs. T (vide supra), the singlet to triplet separation ($2J$) is therefore 21.6 cm^{-1}. The values of kT at 1.9 and 4.3

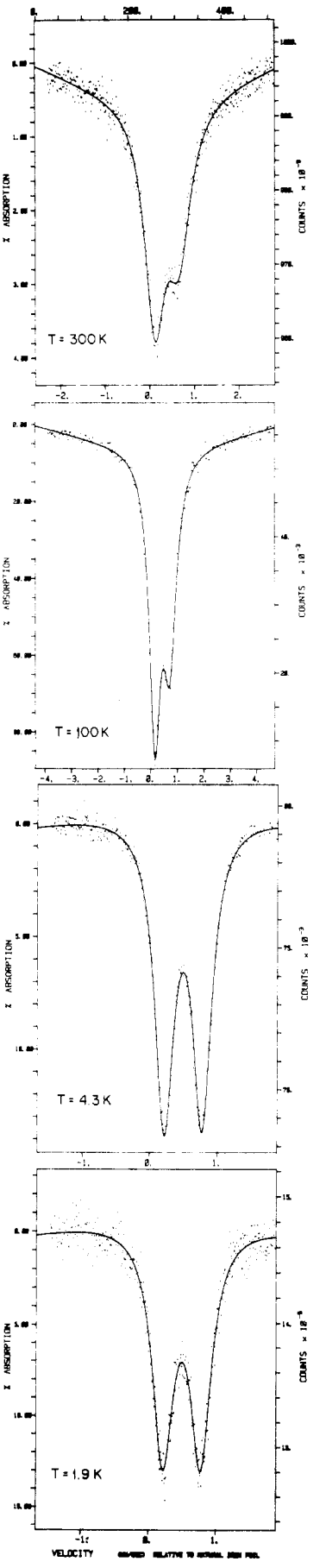

Figure 5. Temperature dependence of Mössbauer spectra of $[FeLOH]_2 \cdot 2H_2O \cdot 2py$.

(12) Greenwood, N. N.; Gibb, T. C. "Mössbauer Spectroscopy"; Chapman and Hall: London, 1971; p 162.
(13) Reiff, W. M.; Long, G. J.; Baker, W. A., Jr. *J. Am. Chem. Soc.* **1968**, *90*, 6347.
(14) Reiff, W. M. *J. Chem. Phys.* **1971**, *54*, 4718.
(15) Murray, K. S. *Coord. Chem. Rev.* **1974**, *12*, 1–35.
(16) Gerloch, M.; Mabbs, F. E. *J. Chem. Soc. A* **1967**, 1900.

K are ~1.6 and 2.9 cm^{-1}, respectively. There is thus little population of the first excited $S_T = 1$ and higher S_T states. Hence the symmetric doublet spectrum observed at the preceding temperatures is as expected for an essentially diamagnetic ($S_T = 0$) ground state. That is, for this state there can be neither magnetic hyperfine splitting nor slow paramagnetic relaxation from zero-field splitting.[14] As the temperature increases, one sees distinct line width asymmetry that we attribute to zero-field splitting of the higher ($S_T = 1, 2, 3, 4, 5$) total spin states of the dimer that are now populated and *slow interdimer* spin–spin relaxation. The *intradimer* spin–spin relaxation is expected to be rapid owing to the small metal–metal distance (~3.2 Å) and exchange. On the other hand, the interdimer metal–metal separations are substantially larger (shortest Fe–Fe distance ~7.073 Å), leading to slow spin–spin relaxation between the excited S_T states of different dimer units. In view of the ^6A ground state of the individual Fe^{3+} ions, we do not consider spin–*lattice* relaxation to be important in the present context.

Another effect evident as the temperature increases is the growth of area symmetry, i.e., $A_1/A_2 \neq 1$. This can be attributed to anisotropy of the recoil-free fraction (Goldanskii–Karyagin effect).[17] This, in turn can be related to the anisotropy of the chemical bonding at the metal ion sites. The latter is clearly evident, for instance, in the nonequivalent diol bridge bonds. As the temperature is decreased and the most symmetric (A_1 irreducible representation) vibrational state of the system is populated, the foregoing effect is expected to vanish, leading to $A_1/A_2 \rightarrow 1$. The value of this ratio at room temperature is the same for finely ground vs. unpulverized samples, suggesting that the origin of the area asymmetry is not sample texture. However, to be sure of this point, one would have to prepare an unoriented absorber by support or dilution in silica or alumina and then determine the temperature dependence of its spectrum, a study beyond the scope of the present investigation. Finally we point out that the related dimer $[Fe(salen)Cl]_2$ exhibits a temperature-dependent asymmetry in its Mössbauer spectrum that is very similar to that observed here and that is likewise explicable primarily as the result of slow interdimer spin–spin relaxation and to a lesser extent recoil-free fraction anisotropy.[18,19]

Discussion

Binuclear iron(III) complexes continue to be of interest because of the biological implications of polynuclear iron complexes.[1,15] Several monoalkoxy and dialkoxy-bridged iron(III) complexes have been reported with a variety of ligands containing oxygen and nitrogen donor atoms; however, fewer dihydroxy-bridged dimers of iron(III) have been reported. One type of ligand that has been used in several studies of iron is the Schiff base salen. In the iron(III) complexes of salen that are reported,[2-5] the salen ligands adopt geometries in which each salicylaldimine group is approximately planar (as predicted); however, a puckering of the entire molecule can occur. Three of the iron(III) complexes exemplify the general types of salen complexes that have been reported: [Fe(salen)Cl], a monomeric five-coordinate complex, $[Fe(salen)Cl]_2$, a six-coordinate dioxo-bridged dimer that is "parallel puckered", and $[(Fe(salen))_2O]\cdot 2py$, a five-coordinate oxo-bridged dimer.

The ligand used in this study is the hydrogenated form of salen, referred to as H-salen. Since the nitrogen atoms in this ligand are sp^3 hybridized, one might expect a greater degree of flexibility and possible deviations from planarity of the ligand when it binds to a metal atom. We report here the preparation of a dihydroxy-bridged complex in which distorted-octahedral symmetry is observed for the iron(III) ions, the result of nonplanarity in the ligands. We assume that a five- or six-coordinate monomeric iron species is present in solution and that only upon addition of water were hydroxide ions available and therefore precipitation of the dimeric compound was made possible. Salen was used in the same synthetic procedures, and an oxo-bridged dimer was obtained rather than the dihydroxy dimer as observed for H-salen. Magnetic data was identical with that previously reported.[4]

Schugar and co-workers have synthesized and characterized some dihydroxy-bridged iron(III) complexes using pyridine-2-carboxylate and two of its derivatives.[20,21] This ligand is a three-electron-pair donor so a molecule of water as well as the two hydroxy groups are required to complete the six coordination sites on the iron ions. In Table VII a list of bond lengths and bond angles of some iron(III) dimers is presented, including the dihydroxy-bridged complexes prepared by Schugar and co-workers as well as some of the complexes of salen that have been reported. The bond distances and the bond angles of the three dihydroxy-bridged dimers are very similar, and there are no apparent differences between the N_2O_2 and the N_1O_3 ligands.

The characteristic vibrational energies of polynuclear iron(III) structural units are usually found at ~850 cm^{-1} (asymmetric) and 230 cm^{-1} (symmetric) for the Fe–O–Fe unit

Table VII. Bond Lengths and Bond Angles for Some Iron(III) Dimers

compd	Fe–Fe, Å	Fe–O, Å	Fe–O–Fe, deg
$[FeLOH]_2\cdot 2H_2O\cdot 2py$	3.155	2.055 (6) 1.986 (6)	102.8 (3)
$[Chel(H_2O)FeOH]_2$	3.078	1.938 (4) 1.989 (4)	103.2 (2)
$[Dipic(H_2O)FeOH]_2$	3.089	1.938 (5) 1.993 (5)	103.6 (2)
$[(Fe(salen))_2O]$	3.37	1.820	139
$(enH_2)[((HEDTA)Fe)_2O]\cdot 6H_2O$		1.8	165
$[Fe(salen)Cl]_2$	3.29	1.98 2.18	95
$[Fe(SALPA)(SALPAH)]_2$	3.217	1.93 (2) 2.00 (2)	108.2 (9) 110.6 (9)

Table VIII. Vibrational Mode in the 800–1000-cm^{-1} Region for Various Iron(III) Dimers

compd[a]	freq, cm^{-1}	ref
$[FeLOH]_2\cdot 2H_2O\cdot 2py$	880	this work
$[Fe(C_4O_4)(H_2O)_2(OH)]_2\cdot 2H_2O$	850	22
$[Chel(H_2O)FeOH]_2$	900	10
$[Dipic(H_2O)FeOH]_2$	900	10
$[(pic)_2FeOH]_2$	947	20
$[(HEDTA)Fe]_2O^{2-}$	840	20
$(enH_2)[((HEDTA)Fe)_2O]\cdot 6H_2O$	857	20

[a] Abbreviations: L = *N,N'*-ethylenebis(salicylamine); Chel = 4-hydroxy-2,6-pyridinedicarboxylate; Dipic = 2,6-pyridinedicarboxylate; pic = pyridine-2-carboxylate; HEDTA = hydroxyethylenediaminetriacetate; C_4O_4 = squarate.

(17) Karyagin, S. V. *Dokl. Akad. Nauk. SSSR* **1963**, *148*, 1102.
(18) Buckley, A. N.; Wilson, G. V. H.; Murray, K. S. *Solid State Commun.* **1969**, *7*, 471.
(19) Buckley, A. N.; Herbert, I. R.; Rumbold, B. D.; Wilson, G. V. H. Murray, K. S. *J. Phys. Chem. Solids* **1970**, *31*, 1423.
(20) Schugar, H.; Rossman, G. R.; Gray, H. B. *J. Am. Chem. Soc.* **1969**, *91*, 4564.
(21) Lippard, S. J.; Schugar, H. J.; Walling, C. *Inorg. Chem.* **1967**, *6*, 1825.
(22) Wrobleski, J. T.; Brown, D. B. *Inorg. Chim. Acta* **1979**, *35*, 109.
(23) Hoffman, A. B.; Collins, D. M.; Day, V. W.; Fleisher, E. B.; Srivastana, T. S.; Hoard, L. H. *J. Am. Chem. Soc.* **1972**, *94*, 3620.
(24) Fleisher, E. A.; Palmer, J. M.; Srivastana, T. S.; Chatteijee, A. *J. Am. Chem. Soc.* **1971**, *93*, 3162.
(25) Borer, L. L.; Vanderbout, W. *Inorg. Chem.* **1979**, *18*, 526.
(26) Bertrand, A.; Eller, P. G. *Inorg. Chem.* **1974**, *13*, 927.
(27) Pure, R. N.; Asplund, R. O. *J. Coord. Chem.* **1981**, *11*, 73.
(28) Wu, C. S.; Rossman, G. R.; Gray, H. B.; Hammond, G. S.; Schugar, H. J. *Inorg. Chem.* **1972**, *11*, 990.

Table IX. Exchange Interactions in Some Iron(III) Mono- and Dibridged Complexes

compd	room temp μ_{eff}, μ_B	J, cm^{-1}	ref
Dihydroxy Complexes			
$[FeLOH]_2$	5.54	−6.9	this work
$[FeLOH]_2 \cdot 2H_2O \cdot 2py$	5.17	−10.4	this work
$[Chel(H_2O)FeOH]_2$	5.24	−7.3	10
$[Dipic(H_2O)FeOH]_2$	4.86	−11.4	10
$[(pic)_2FeOH]_2$	5.10	−8.0	20
$[Fe(C_4O_4)(py)_2(OH)]_2 \cdot 2H_2O$	5.22	−7.0	22
$[Fe(C_4O_4)(4\text{-Mepy})_2(OH)]_2 \cdot 2H_2O$	5.19	−8.6	22
$[Fe(C_4O_4)(3\text{-Mepy})_2(OH)]_2 \cdot 2H_2O$	5.24	−7.8	22
Monooxo Complexes			
$(enH_2)[((HEDTA)Fe)_2O] \cdot 6H_2O$	1.90	−95	21
$[Fe(salen)]_2O \cdot py$		−90	3
$[Fe(salen)_2]O$	1.89	−95	4
$[Fe(TPP)]_2O$	1.86	−100	23, 24
Dialkoxy Complexes			
$[Fe(salen)Cl]_2$	5.36	−7.5	5
$[Fe(DBA)(H_2O)(OH)]_2$	4.50	−17.8	25
$[Fe(SALPA)(SALPAH)]_2$	4.45	−8.0	26
$[(L\text{-proline})Fe(OCH_3)(H_2O)]_2$	4.34	−8.5	27
$[(DPM)_2Fe(OCH_3)]_2$	5.09	−8.5	28
$[(acac)_2Fe(OC_2H_5)]_2$	4.95	−11.0	28
***p*-Quinone Complexes**			
$[Fe(salen)]_2Q$	5.38	−2.5	29
$[Fe(salen)]_2ClQ$	5.61	−2.0	29
$[Fe(salen)]_2DuQ \cdot THF$	5.30	−4.0	29

as shown by ^{18}O experiments.[15] A weak band at ~950 cm^{-1} has been shown by deuteration experiments to be due to OH bridging deformation in an $[Fe-(OH)_2-Fe]^{4+}$ unit. Since there are several ligand bands in the 900–700-cm^{-1} region of the IR spectra that would obscure any peaks arising from ^{18}O substitution, this experiment was not done. However, upon deuteration, the 880-cm^{-1} peak diminished while another was observed at ~620 cm^{-1}, making it possible to assign the 880-cm^{-1} peak to the OH bridging deformation. This assignment agrees with assignments reported for a representative group of μ-dihydroxy-bridged dimers as shown in Table VIII.

The extent of antiferromagnetism exhibited by various mono- and dibridged iron(III) complexes as shown by the exchange integral, J, are given in Table IX. The Fe–Fe separation of all compounds is large enough so that any direct overlap of metal atom orbitals can be neglected; therefore, only a superexchange mechanism via the ligand atoms is important. It is apparent from the data that all dihydroxy-bridged dimers have essentially the same degree of exchange, ~10 cm^{-1}. They do not differ substantially from the dialkoxy-bridged dimers except, for example, in $[Fe(DBA)(H_2O)(OH)]_2$, where the basicity of the ligand appears to be important and the exchange constant has somewhat increased (~20 cm^{-1}). The number of bridging atoms is also important. Monooxo-bridged iron(III) dimers exhibited, in general, a shorter Fe–O–Fe bond distance and a greater degree of linearity; therefore, they exhibit a greater degree of exchange with $J \cong 100$ cm^{-1}. As expected, Hendrickson and Kessel[29] have shown that extending the number of bridging atoms between the two iron ions, for example, by using a *p*-quinone group as the bridging species, results in a substantial reduction in the exchange.

Acknowledgment. Fellowship support to C.C. by NSF Contract No. CHE 8010809 and to L.B. by a Faculty Research Grant are gratefully acknowledged.

W.M.R. wishes to acknowledge the support of the National Science Foundation, Division of Materials Research, Solid State Chemistry Program (Grant No. DMR-80-16441).

Registry No. $[Fe(C_{16}H_{18}N_2O_2)OH]_2$, 85369-98-8; $[Fe(C_{16}H_{18}N_2O_2)OH]_2 \cdot 2H_2O \cdot 2py$, 85439-52-7; $[Fe(C_{16}H_{18}N_2O_2)OH]$-$d_6$, 85369-99-9.

Supplementary Material Available: Listings of positional and thermal parameters for hydrogen atoms, thermal parameters for non-hydrogen atoms, and observed and calculated structure factors (12 pages). Ordering information is given on any current masthead page.

(29) Kessel, S. L.; Hendrickson, D. N. *Inorg. Chem.* **1978**, *17*, 2630.